water

MDPI

Article

Optimization Analysis to Evaluate the Relationships between Different Ion Concentrations and *Prymnesium parvum* Growth Rate

Shuang-Yu Liu [1], Rui-Zhi Zhao [1], Xiao-Cong Qiu [2,*] and Qi Guo [3]

[1] School of Civil and Hydraulic Engineering, Ningxia University, Yinchuan 750021, China; liushuangyu1999@163.com (S.-Y.L.); takuinugalaxy@sina.com (R.-Z.Z.)
[2] School of Life Science, Ningxia University, Yinchuan 750021, China
[3] Xinjiang Corps Survey and Design Institute (Group) Co., Ltd., Wulumuqi 830002, China; gq787937@163.com
* Correspondence: qiu_xc@nxu.edu.cn

Abstract: The purpose of this study was to evaluate the optimum environmental condition required for reaching the maximum growth rate of *P. parvum*. Eight ions (Na^+, K^+, CO_3^{2-}, HCO_3^-, Ca^{2+}, Mg^{2+}, Cl^-, and SO_4^{2-}) were divided into two groups with a uniform design of 4 factors and 10 levels. The results showed a rising trend in growth rate with increasing ion concentrations. However, concentrations that exceeded the threshold led to a slowdown in the growth rate. Therefore, adequate supply of ion concentrations promoted growth of *P. parvum*, whereas excessively abundant or deficient ion concentrations inhibited its growth rate. Specifically, the order of impact of the first four ion factors on the growth rate was $Na^+ > HCO_3^- > K^+ > CO_3^{2-}$. The growth rate of *P. parvum* reached the maximum theoretical 0.999 when the concentrations of Na^+, K^+, CO_3^{2-}, and HCO^{3-} ions were 397.98, 11.60, 3.37, and 33.31 mg/L, respectively. This theoretical growth maximum was inferred from the experimental results obtained in this study. For other ion factors, SO_4^{2-} had the most influence on the growth rate of *P. parvum*, followed by Mg^{2+}, Ca^{2+}, and Cl^- ions. The growth rate of *P. parvum* reached the maximum theoretical value of 0.945 when the concentrations of Ca^{2+}, Mg^{2+}, Cl^-, and SO_4^{2-} ions were 11.52, 32.95, 326.29, and 377.31 mg/L, respectively. The findings presented in this study add to our understanding of the growth conditions of *P. parvum* and provide a theoretical basis for dealing with the water bloom it produces in order to control and utilize it.

Keywords: uniform design; ion conditions; regression model; optimization; growth rate; *Prymnesium parvum*

Citation: Liu, S.-Y.; Zhao, R.-Z.; Qiu, X.-C.; Guo, Q. Optimization Analysis to Evaluate the Relationships between Different Ion Concentrations and *Prymnesium parvum* Growth Rate. *Water* **2022**, *14*, 928. https://doi.org/10.3390/w14060928

Academic Editor: Wenhui Gu

Received: 21 January 2022
Accepted: 11 March 2022
Published: 16 March 2022

1. Introduction

P. parvum is a single-celled microalgae that has the potential to cause massive fish kills [1,2]. This microalgae is suitable for growth in water with a salinity of 0.6–70.0‰, with the optimum salinity being 3.0–5.0‰. Water temperature of about 20 °C is the most suitable condition for its growth. Under some situations, the concentration of ichthyotoxins secreted by *P. parvum* can kill fish, causing ecological damage [3–5]. These toxins have been shown to have potent protease and hemolytic properties [5]. At certain concentrations, the toxin, which is dominated by chemicals known as "prymnesins", can be fatal to gill-breathing species, such as fish [6]. In high-salinity water bodies, *P. parvum* can easily reproduce. In ponds and ditches in saline areas of northern China, such algae can easily reach optimum growth conditions, and the toxins they secrete cause mass mortality of cultured fish in this area [7].

The microalgae growth rate is closely related to ion concentrations in the solution environment. The relationship between algal growth and ion concentration has been studied in *Chlorella*, *Tetrahymena*, and *Microcystis aeruginosa* [8,9]. However, no research has been conducted on *P. parvum*, which is a common species in saline areas in northern

China, particularly in Ningxia, and the goal of this paper is to do so. Different ions have distinct effects on microalgae. Metal ions, particularly Al^{3+}, Ca^{2+}, Fe^{2+}, and Mg^{2+} ions, can promote the growth rate of microalgae. Hence, microalgae are cultivated using industrial wastewater to purify water [10]. The concentrations of carbon, nitrate, and magnesium are 10.000, 15.000, and 150 mg/L, respectively, showing the maximum biomass growth rate of microalgae [11]. The optimal concentrations of KNO_3, $CO(NH_2)_2$, and $NaHCO_3$ for microalgae growth rate are 500, 360, and 1500 mg/L, respectively [12]. In reality, ions have more than just facilitative impacts on microalgae. $SO_4{}^{2-}$ ions can cause toxins to accumulate in microalgae cells [13], while Cl^- ions can effectively reduce the cell density and chlorophyll-a of microalgae [14]. Pb^{2+} ions have been shown to have toxic effects on two microalgae [15], and Cd^{2+} ions at a concentration of 7 mg/L was found to inhibit microalgae growth rate [16]. Furthermore, the ion concentration influences the growth of microalgae, either inhibiting or promoting it [17–20]. It is clear that ion concentration and microalgae growth rate have a complicated relationship. To a certain extent, the interaction between various ions will affect the growth rate of microalgae. As a result, an optimal ion concentration will boost microalgae biomass.

Waters in the Ningxia region of China, particularly in Yinchuan and North of Yinchuan areas, have a high salt alkalinity (pH ranges from 7.8 to 9.2). As a result, during the cooler seasons, when the temperature suitable for *P. parvum* growth can reach around 18 °C, *P. parvum* can multiply in large outbreaks, releasing more toxins and affecting fish growth. This can result in a sharp decline in the ecological environment and have a negative impact on the economic development of fisheries. There is currently very little published information on the growth characteristics of *P. parvum* and how the ionic factor impacts its growth rate. In the present study, a uniform design (UD) method [21–23] was used to quantify the effects of ion concentration (Na^+, K^+, $CO_3{}^{2-}$, $HCO_3{}^-$, Ca^{2+}, Mg^{2+}, Cl^-, and $SO_4{}^{2-}$) on the growth rate of *P. parvum*. By constructing growth curves with each ion factor, we were able to estimate the optimum growth conditions for *P. parvum.* By studying the physiological characteristics of the growth rate of this environmentally harmful microalgae, we discuss the optimal growth rate as influenced by ionic factor conditions.

2. Materials and Methods

2.1. Purification and Culture of P. parvum

In October 2019, the experimental microalgae *P. parvum* was collected from fish ponds in Dawukou, Ningxia, China. After sampling, we brought them back to the laboratory for isolation, culture, and expansion in preparation for the ion concentration test. After centrifugation, microalgal water samples were incubated in F/2 medium (the composition of which is shown in Table 1) for five days, with the light intensity set to 5000 lux, light/dark ratio set to 12 h:12 h, the temperature set to 18.5 ± 0.5 °C, the pH set to 8.5 ± 0.1, and the salinity set to 1.2 ± 0.1 mg/L. Water samples were filtered using filter paper. In this case, centrifugation was carried out at 2600 rpm for one minute while the temperature was kept at 20.5 ± 0.5 °C. The solution was concentrated, and the supernatant was discarded before incubating. This light time was used in this study for all cultures.

P. parvum was isolated using the plate method. A suitable amount of microalgal seeds was inoculated on a solid medium and cultured in the aforementioned environmental conditions, with the growth rate condition checked by microscopic examination once per day. The composition and content of the solid medium were as follows [24]: $CO(NH_2)_2$ (42.4 mg), KH_2PO_3 (8 mg), $FeC_6H_5O_7$ (1 mg), Na_2SiO_3 (10 mg), VB_1 (200 mg), VB_{12} (1 mg), $NaHCO_3$ (500 mg), agar (6 g), potassium sorbate (25 mg), and EDTA-Na (2 mg). After 10 days, the colony of pure microalgal cells was transferred to 50 mL triangular flasks containing a sterilization medium to expand the culture. These microalgal strains were inoculated in 250 mL triangular glass bottles with F/2 medium in the above environmental conditions. When the microalgal cells had reached the logarithmic growth period (approximately 10 days), they were inoculated in a 10 L triangular glass bottle containing expansion culture. During the culture test, cell counts were obtained every 24 h. Continuous observa-

tion was carried out until the cell count stopped increasing. The logarithmic growth period of this algal cell was about 10 days. Solid medium was utilized to extract and purify the small trichogramma golden algae without counting CFU. The liquid medium was used for expansion and counting analysis using the ion impact test. These proliferated microalgae were used as test materials for the study.

Table 1. F/2 medium composition.

Raw Material	Content (mg/L)	Component	Content (mg/L)
NaCl	363.84	Ca	17.05
Na_2S0_4	382.66	Mg	35.47
$MgS0_4$	177.35	Na	434.46
K_2S0_4	34.49	K	15.46
$CaCl_2$	47.31	$C0_3{}^{2-}$	3.31
Na_2CO_3	5.85	$HC0_3{}^{-}$	36.4
$NaHC0_3$	50.12	Cl-	251.05
$NaN0_3$	20.7	$S0_4{}^{2-}$	419.61
NaH_2PO_4	4.06	N	3.41
Na_2SiO_3	3.01	P	1.05
$FeC_6H_5O_7$	2.32	Si	0.69

2.2. Experimental Design

We used a uniform design, a new experimental design method based on the quasi-Monte Carlo method proposed by the mathematician Fang Kaitai [25]. This method can effectively reduce the number of experimental tests and is more suitable for use in multidimensional space- and data-limited situations [26]. Satisfactory results can be obtained with a smaller number of trials. Uniform design can not only overcome the disadvantage of a single-factor test, which does not consider the interaction between factors, but also solves the problem of fewer factors in orthogonal tests. A consistent design enables selection of the most representative test sites within the test range [21]. When the number of trials is the same, a multilevel setting can be performed so that the range of trials for each factor can be further investigated and the test factors can be automatically categorized. Because uniform design is currently effectively used in the optimization of microalgal culture conditions, it was chosen as the experimental theoretical basis for this study [27]. In this study, the test sites were the various ions chosen, and the test range for each factor was the ion concentration range.

The scheme was optimized using distributed parameter systems (DPS) homogeneous design software as well as multifactor and square term regression analysis. The eight ions were divided into two groups, and the effect of different ion concentrations on the optimal growth rate of *P. parvum* was determined using a uniform design with 4 factors and 10 levels with a $U^*_{10}(10^4)$ homogeneous design table.

Table 2 shows the established levels of the experimental factors for group 1, namely sodium ion (Na^+), potassium ion (K^+), carbonate ion ($CO_3{}^{2-}$), and bicarbonate ion ($HCO_3{}^{-}$). The experimental treatment was divided into 10 groups, with each group receiving three parallel samples (30 bottles in total). The specific ion content measured in the field environment of the water for microalgae growth was as follows: Na^+ 397.9 mg/L, K^+ 14.11 mg/L, $C0_3{}^{2-}$ 5.6 mg/L, $HC0_3{}^{-}$ 37.0 mg/L, Ca^{2+} 14.46 mg/L, Mg^+ 45.85 mg/L, Cl^- 300.0 mg/L, and $S0_4{}^{2-}$ 460 mg/L. The ion concentration range influencing the growth of *P. parvum* was finally determined by referring to related research results of other scholars [28–31].

Similarly, Table 3 shows the established levels of the experimental factors for group 2, namely calcium ion (Ca^{2+}), magnesium ion (Mg^{2+}), chloride ion (Cl^-), and sulfate ion ($SO_4{}^{2-}$). The experimental design was identical to that of group 1.

Table 2. Experimental factors (Na^+, K^+, CO_3^{2-}, and HCO_3^- ions) and established levels.

Experiment Number	Levels of Experimental Factors			
	Na^+	K^+	CO_3^{2-}	HCO_3^-
	X_1 (mg/L)	X_2 (mg/L)	X_3 (mg/L)	X_4 (mg/L)
1	250	9	9	20
2	550	6	2	55
3	650	12	5	25
4	400	3	7	35
5	350	27	1	30
6	300	24	6	60
7	200	15	3	45
8	500	21	4	15
9	450	18	10	50
10	600	30	8	40

Table 3. Experimental factors (Ca^{2+}, Mg^+, Cl^-, and $S0_4^{2-}$ ions) and established levels.

Experiment Number	Levels of Experimental Factors			
	Ca^{2+}	Mg^+	Cl^-	$S0_4^{2-}$
	X_5 (mg/L)	X_6 (mg/L)	X_7 (mg/L)	X_8 (mg/L)
1	6	25	550	250
2	24	20	200	600
3	30	30	350	300
4	15	15	450	400
5	12	55	150	350
6	9	50	400	650
7	3	35	250	500
8	21	45	300	200
9	18	40	600	550
10	9	60	500	450

2.3. Culture Methods and Conditions

A 250 mL triangular glass bottle was used for the experiment (60 bottles in total). The basic nutrient solution was F/2 medium, and the volume of the nutrient solution was 100 mL with an inoculation ratio of 1:10 (%, v/v). The light incubation conditions of the medium were light intensity of 5000 lux and light/dark ratio of 12 h:12 h. Eight samples were treated in the manner shown in Tables 1 and 2, with three replicates for each treatment. The average value of repeated treatments was used as a parameter. The samples were cultured in a constant temperature and light culture shaker for 10 days (oscillation frequency 100 rpm and temperature range 18.0 ± 0.5), with counting proceeding after the exponential growth rate period.

2.4. Determination of Microalgal Growth Rate

The cell density of the samples was calculated under a light microscope using a hemocytometer plate made of 0.1 mL high-quality thick glass (0.10 mm, 1/400 mm^2, Changde Bkmam Biotechnology Co., Ltd., Changde, China). After incubation for 10 days, the growth rate of the microalgal reached the exponential growth period. From the 10th day onwards, sample counts were started so that the growth rate of *P. parvum* could be determined. The growth rate of microalgae cells can be calculated according to the following equation [32]:

$$\text{Growth rate (K)} = 3.322 \times (\log(N_t) - \log(N_0))/(t - t_0) \quad (1)$$

where t is the duration of the experiment, N_0 is the initial cell density before the experiment, and N_t is the cell density at day t of the experiment. This is the growth rate as a function of polymeric ion concentration (i.e., salinity) [33].

2.5. Data Analysis

The multifactor test method and multiple regression analysis were used to reduce the number of tests using a homogeneous design. Using the optimized scheme, regression equations were established for the growth rate of *P. parvum* with Na^+, K^+, CO_3^{2-}, HCO_3^- Ca^{2+}, Mg^{2+}, Cl^-, and SO_4^{2-} ion factors. Excel 2013 and DPS v17.10 statistical analysis software were used to conduct multiple regression analysis of data, and OriginPro 2019a software was used to draw a graph of the obtained model.

3. Results and Analysis

3.1. Establishment of the Regression Model of Na^+, K^+, CO_3^{2-}, HCO_3^-, and Growth Rate

The results of the relationship between *P. parvum* growth rate and Na^+, K^+, CO_3^{2-}, and HCO_3^- concentrations are shown in Table 4.

Table 4. Results of the growth rate of *P. parvum* under different concentrations of Na^+, K^+, CO_3^{2-}, and HCO_3^-.

Experiment Number	Experimental Factors				Experimental Parameters
	Na^+	K^+	CO_3^{2-}	HCO_3^-	Growth Rate
	X_1	X_2	X_3	X_4	Y_1 (Cell/d)
1	250	9	9	20	0.417
2	550	6	2	55	0.591
3	650	12	5	25	0.669
4	400	3	7	35	0.644
5	350	27	1	30	0.638
6	300	24	6	60	0.515
7	200	15	3	45	0.447
8	500	21	4	15	0.391
9	450	18	10	50	0.644
10	600	30	8	40	0.555

A quadratic polynomial regression equation was generated using Na^+ (X_1), K^+ (X_2), CO_3^{2-} (X_3), and HCO_3^- (X_4) as independent variables and growth rate (Y_1) as the dependent variable using multiple quadratic stepwise regression analyses:

$$Y_1 = -45.4705 + 27.4436\log X_1 + 1.6676\log X_2 + 0.8747\log X_3 + 12.7100\log X_4 - 5.2779(\log X_1)^2 - 0.7832(\log X_2)^2 - 0.8289(\log X_3)^2 - 4.1737(\log X_4)^2$$

By partial correlation analysis, the partial correlation coefficients of *P. parvum* growth rate and variables X_1, X_2, X_3, and X_4 were 0.9992, 0.9990, 0.9981, and 0.9995, respectively, with p-values of 0.03, 0.03, 0.04, and 0.02, respectively, indicating that the *P. parvum* growth rate was significantly correlated with variables X_1, X_2, X_3, and X_4. The r-value of the regression equation was 0.9997, and the p-value of the F-test was 0.036 (<0.05), indicating that the regression relationship between Na^+, K^+, CO_3^{2-}, HCO_3^-, and *P. parvum* growth rate was significant. The model was consistent with the experimental data (Table 4), thereby strongly reflecting the relationship between Na^+, K^+, CO_3^{2-}, HCO_3^-, and the growth rate of *P. parvum*.

The standardized regression coefficients of the factors in the regression equation and the optimal combination of the experimental factors are shown in Table 5. The experimental conditions that would promote the growth rate of *P. parvum* were determined by optimizing the regression equation Y_1.

The growth rate reached the maximum theoretical value of 0.999 when the Na^+, K^+, CO_3^{2-}, and HCO_3^- concentrations were 398.02, 11.60, 3.37, and 33.31 mg/L, respectively.

Table 5. The standardized regression coefficients of the model and optimal combination.

Factors	Na^+	K^+	CO_3^{2-}	HCO_3^-
	X_1	X_2	X_3	X_4
Standardized regression coefficients	44.9493	5.1378	2.6947	24.3353
Growth rate (Y_1 = 0.999)	398.02	11.60	3.37	33.3

3.2. Mathematical Models of the Relationships between P. parvum Growth Rate and Individual Factors (Na^+, K^+, CO_3^{2-}, and HCO_3^-)

A multifactor and square stepwise regression model was used to analyze the influence of a single factor after dimensionality reduction. To easily analyze the influence of a single factor on the growth rate, a submodel of the relationship between every single factor and the growth rate was obtained by fixing other factors at the optimal level.

$$Na^+: Y(X_1) = -34.6758 + 27.4436\log X_1 - 5.2779(\log X_1)^2 \quad (2)$$

$$K^+: Y(X_2) = 0.1113 + 1.6676\log X_2 - 0.7832(\log X_2)^2 \quad (3)$$

$$CO_3^{2-}: Y(X_3) = 0.7682 + 0.8747\log X_3 - 0.8289\ (\log X_3)^2 \quad (4)$$

$$HCO_3^-: Y(X_4) = -8.6773 + 12.7100\log X_4 - 4.1737(\log X_4)^2 \quad (5)$$

The influence curves of every single factor on the growth rate are shown in Figure 1. The effect of various factors on growth rate was similar to what is shown in Figure 1.

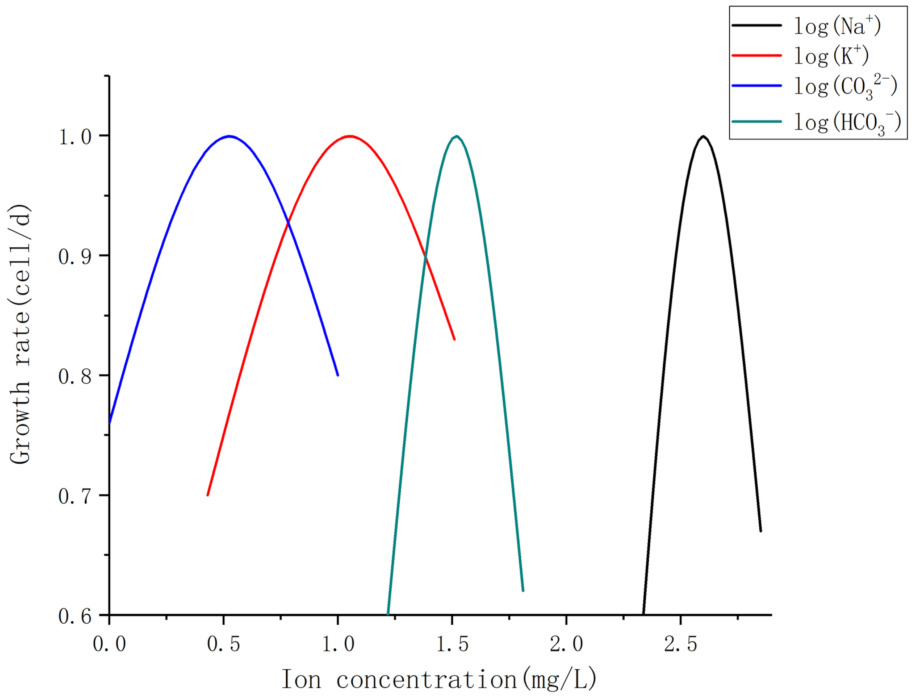

Figure 1. The influence curves of ion conditions on growth rate (Na^+, K^+, CO_3^{2-}, and HCO_3^-).

When the concentration was low, each factor had a positive effect on the growth rate, which was under the effect of the main model. The contribution of the quadratic term became more and more important with the increase in the independent variable. When the independent variable exceeded a certain value, the single factor changed the growth rate to a negative effect. The growth rate of *P. parvum* first increased and then decreased with increasing ion concentrations. The growth rate reached the theoretically highest point of 0.999 with Na^+, K^+, CO_3^{2-}, and HCO_3^- concentrations of 397.98, 11.60, 3.37, and 33.31 mg/L, respectively.

3.3. Establishment of the Regression Model of Ca^{2+}, Mg^{2+}, Cl^{-}, SO_4^{2-}, and Growth Rate

The results of the relationship between *P. parvum* growth and Ca^{2+}, Mg^{2+}, Cl^{-}, and SO_4^{2-} concentrations are shown in Table 6.

Table 6. Results of the growth rate of *P. parvum* under different concentrations of Ca^{2+}, Mg^{2+}, Cl^{-}, and SO_4^{2-}.

Experiment Number	Experimental Factors				Experimental Parameters
	Ca^{2+}	Mg^{+}	Cl^{-}	$S0_4^{2-}$	Growth Rate
	X_5	X_6	X_7	X_8	Y_2 (Cell/d)
1	6	25	550	250	0.605
2	24	20	200	600	0.419
3	30	30	350	300	0.691
4	15	15	450	400	0.470
5	12	55	150	350	0.675
6	9	50	400	650	0.520
7	3	35	250	500	0.468
8	21	45	300	200	0.413
9	18	40	600	550	0.692
10	9	60	500	450	0.626

The quadratic polynomial regression equation generated using Ca^{2+} (X_5), Mg^{2+} (X_6), Cl^{-} (X_7), and SO_4^{2-} (X_8) concentrations as independent variables and growth rate (Y_2) as the dependent variable is as follows:

$$Y_2 = -46.7636 + 2.4173\log X_5 + 11.4688\log X_6 + 3.3727\log X_7 + 25.9886\log X_8 - 1.1389(\log X_5)^2 - 3.7780(\log X_6)^2 - 0.6709(\log X_7)^2 - 5.0430(\log X_8)^2 \quad (6)$$

By partial correlation analysis, the partial correlation coefficients of *P. parvum* growth rate and variables X_5, X_6, X_7, and X_8 were 0.9987, 0.9994, 0.9878, and 0.9997, respectively, with *p*-values of 0.03, 0.02, 0.04, and 0.07, respectively, indicating that the *P. parvum* growth rate was significantly correlated with variables X_5, X_6, X_7, and X_8. The *r*-value of the regression equation was 0.9997, and the *p*-value of the F-test was 0.036 (<0.05), indicating that the regression relationship between Ca^{2+}, Mg^{2+}, Cl^{-}, SO_4^{2-}, and *P. parvum* growth rate was significant. The model fit the data well (Table 6), and the regression model reflected the relationship between Ca^{2+}, Mg^{2+}, Cl^{-}, SO_4^{2-}, and *P. parvum* growth rate. The standardized regression coefficients for each factor in the regression equation were as follows: Ca^{2+} 6.5372, Mg^{2+} 20.1762, Cl^{-} 5.9333, and SO_4^{2-} 39.1108.

By optimizing the regression equation Y_2, the optimal growth rate condition of *P. parvum* was derived. The optimal combination of each experimental factor is given in Table 7.

Table 7. The standardized regression coefficients of the model and optimal combination.

Factors	Ca^{2+}	Mg^{2+}	Cl^{-}	SO_4^{2-}
	X_5	X_6	X_7	X_8
Standardized regression coefficients	6.5372	20.1762	5.9333	39.1108
Growth rate (Y_2 = 0.945)	11.52	32.95	326.29	377.31

The growth rate of *P. parvum* reached the maximum theoretical value of 0.945 when the Ca^{2+}, Mg^{2+}, Cl^{-}, and SO_4^{2-} concentrations were 11.52, 32.95, 326.29, and 377.31 mg/L, respectively.

3.4. Mathematical Models of the Relationships between P. parvum Growth Rate and Individual Factors (Ca^{2+}, Mg^{2+}, Cl^{-}, and SO_4^{2-})

The following simple regression models revealing the relationship between an individual factor and growth rate (Y) were obtained using dimension reduction analyses in which the other factors were maintained at optimal levels:

$$Ca^{2+}: Y(X_5) = -0.3385 + 2.4173\log X_5 - 1.1389(\log X_5)^2 \quad (7)$$

$$Mg^{2+}: Y(X_6) = -7.7598 + 11.4688\log X_6 - 3.7780(\log X_6)^2 \quad (8)$$

$$Cl^{-}: Y(X_7) = -3.2946 + 3.3727\log X_7 - 0.6709(\log X_7)^2 \quad (9)$$

$$SO_4^{2-}: Y(X_8) = -32.5383 + 25.9886\log X_8 - 5.0430(\log X_8)^2 \quad (10)$$

As we can see from Figure 2 and the dimensionality reduction equation, the growth rate of *P. parvum* first increased and then decreased with increasing ion concentration. The growth rate reached the theoretically highest point of 0.945 with Ca^{2+}, Mg^{2+}, Cl^{-}, and SO_4^{2-} concentrations of 11.51, 32.95, 326.29, and 377.31 mg/L, respectively.

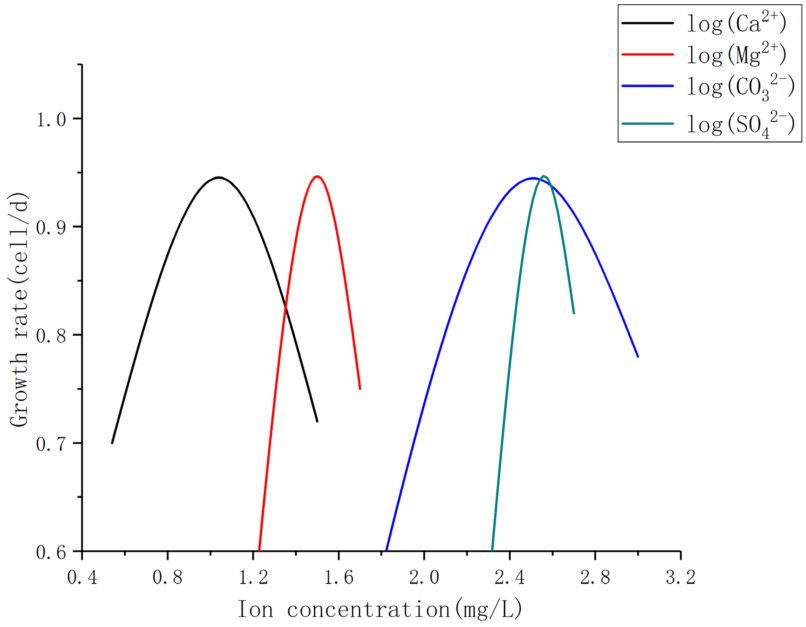

Figure 2. The influence curves of ion conditions on growth rate (Ca^{2+}, Mg^{2+}, Cl^{-}, and SO_4^{2-}).

4. Discussion

By regulating the fluidity of cell membranes, Na^+ ion can maintain the osmotic pressure of algal cells and influence lipid synthesis in the cells. This can change the dynamics of substance exchange across the plasma membranes as well as the solubility of CO_2 and O_2 in the environment, thereby affecting the metabolic rate of algal cells. Microalgae growth can be influenced by K^+ ion. An increase in K^+ ion concentration can cause intracellular Na^+ ion loss, which can raise the pH of microalgae cells. This could then affect the growth and physiological state of the microalgae [34]. Na^+ and K^+ ions are elements necessary for microalgal growth rate. Thus, their concentrations inevitably affect the growth rate of algae. The growth rate of *P. parvum* increased with increasing concentrations of Na^+ and K^+ ions in this study but began to decrease when the respective concentration thresholds were reached. This suggests that too high concentrations of Na^+ and K^+ ions can inhibit the growth rate of *P. parvum*. Furthermore, when the standardized regression coefficients were compared, it was discovered that the effect of Na^+ ion on the growth rate of *P. parvum* was greater than that of K^+ ion.

The growth rate of microalgae depends on inorganic carbon fixation for photosynthesis. Free CO_2 and HCO_3^- can be absorbed and utilized by microalgae as a source of inorganic carbon, whereas CO_3^{2-} is not readily used for photosynthesis in microalgae. As a result, the CO_2 buffer system in the culture medium is essential for the microalgal growth rate. Some algal species, such as *Scenedesmus* sp. [35], *Nannochloropsis salina* [36], and *Chlorella kessleri* [37], can use HCO_3^- ion to support rapid growth. The concentration of $NaHCO_3$ is known to have a significant effect on the growth characteristics of *Isochrysis*. Microalgae might utilize the HCO_3^- ion in the environment via two mechanisms. The first is the transmembrane transport of external HCO_3^- ion into the cytosol, where HCO_3^- ion is decomposed into CO_2 by intracellular carbonic anhydrase enzyme for photosynthesis. The second is the secretion of extracellular carbonic anhydrase enzyme by some microalgae. Carbonic anhydrase speeds the dehydration of HCO_3^- into CO_2. The CO_2 is then transported through the membrane into the microalgal cells [38,39]. As different microalgal species produce carbonic anhydrases enzyme with different enzymatic activities in different locations, their ability to utilize HCO_3^- ion in the environment is also different. The addition of 1000 mg/L of $NaHCO_3$ into the culture medium was found to have the best growth-promoting effect in chlorella (*Chlorella vulagris* ESO-31) [40]. The addition of 0.6 g/L of $NaHCO_3$ to the BG-11 medium increased the biomass of the microalgae *Scenedesmus* [36]. Furthermore, when the $NaHCO_3$ concentration was 1600 mg/L, the maximum abundance of three marine microalgae were obtained. An appropriate amount of $NaHCO_3$ can improve the photosynthetic efficiency of *Tetraselmis suecica* and *N. salina* and promote the absorption of other nutrient salts by microalgal cells [36]. However, excessive $NaHCO_3$ can inhibit the microalgal growth rate [40]. As CO_3^{2-} ion cannot be directly utilized by microalgae, HCO_3^- ion becomes an essential ion for the microalgal growth rate, and its concentration could affect the growth rate of microalgae. Moreover, HCO_3^- and CO_3^{2-} ions and CO_2 together constitute a carbonic–carbonate system in the water, where they can interchange into one form or another under certain conditions. Under alkaline conditions, both carbonate and bicarbonate are readily present, and carbonate is more likely to undergo hydrolysis. In this study, the growth rate of *P. parvum* first increased as the HCO_3^- and CO_3^{2-} ion concentrations increased but then began to decrease when the respective concentration thresholds were reached. This suggests that excessively high concentrations of HCO_3^- and CO_3^{2-} ions could inhibit the growth rate of *P. parvum*. Furthermore, the effects of HCO_3^- ion on the growth rate of *P. parvum* was found to be greater than that of CO_3^{2-} ion based on the standardized regression coefficients of each factor in the growth regression equations.

Ca^{2+} ion is essential for cell division. It plays an important role in the formation of the middle lamella and mitotic spindle during mitosis. Ca^{2+} ion also maintains stability of the cell wall, cell membrane, and membrane-bound proteins and is involved in the regulation of various biochemical processes in the cells. Ca^{2+} ion can regulate the intercellular ion environment and reduce the adverse effects caused by low pH, toxic ions, and nutritional imbalances. Ca^{2+} ion is implicated in the regulation of many physiological processes. It also serves as an important structural element. Ca^{2+} ion can promote plant growth and increase photosynthesis capacity, but a high Ca^{2+} ion concentration might inhibit the growth rate and photosynthesis of microalgae [41]. Mg^{2+} ion is an essential nutrient for plants. Its main function is to act as and participate in photosynthesis in combination with light energy and enzymatic actions. Mg^{2+} ion is also important for protein metabolism. It has a significant effect on the microalgal growth rate. The growth rate of *Microcystis aeruginosa* was significantly inhibited in an Mg^{2+}-depleted environment, whereas a higher mass concentration of Mg^{2+} ion also inhibited its growth rate [42]. The growth rate of *P. parvum* increased with increasing concentrations of Ca^{2+} and Mg^{2+} ions but began to decrease when the respective concentration thresholds were reached. This indicates that too high concentrations of Ca^{2+} and Mg^{2+} ions can inhibit the growth rate of *P. parvum*. Furthermore, by comparing the standardized regression coefficients, it was discovered that the effect of Mg^{2+} ion on the growth rate of *P. parvum* was greater than that of Ca^{2+} ion.

The salinity of a microalgal culture medium is determined by Cl^- ion concentration. Cl^- is the main ion that makes up and affects the salinity of a water body. Each microalgal species has a distinct salinity value required for its optimal growth. Suitable salinity promotes cell growth. In contrast, a salinity value below or above the optimal range for microalgae might affect their osmotic pressure and reduce their solute absorption capacity, resulting in the inhibition of microalgal growth rate [43]. SO_4^{2-} is an intermediate nutrient required for the growth and development of photoautotrophs. Its significance comes right after the three primary nutrients nitrogen, phosphorus, and potassium. An appropriate amount of sulfur can promote rapid growth and reproduction of microalgal cells [44], whereas less sulfur can decrease the protein and carbohydrate contents of microalgae, leading to the accumulation of a large number of lipids [45]. The growth rate of *P. parvum* increased with increasing concentrations of Cl^- and SO_4^{2-} ions but began to decrease when the respective concentration thresholds were reached. This indicates that too high concentrations of Cl^- and SO_4^{2-} ions can inhibit the growth rate of *P. parvum*. Not only that, by comparing the standardized regression coefficients, it was found that the effect of SO_4^{2-} ion on the growth rate of *P. parvum* was greater than that of Cl^- ion.

5. Conclusions

The main goal of the current study was to determine the effect of different ions and concentrations on the growth rate of *P. parvum*. Too high or too low concentrations of the selected eight ions inhibited the growth rate of *P. parvum*. Through the optimization analysis of the growth equation, combined with the numerical simulation of the one-way regression model, we found that the growth rate of *P. parvum* reached the theoretical maximum of 0.999 when the concentrations of Na^+, K^+, CO_3^{2-}, HCO_3^- were 398.02, 11.60, 3.37, and 33.31 mg/L, respectively. Moreover, the Na^+ ion had a greater effect on the growth rate than the three other ions. For Ca^{2+}, Mg^{2+}, Cl^-, and SO_4^{2-} ions, the analysis result showed that the growth rate of *P. parvum* reached the maximum theoretical value of 0.945 when the Ca^{2+}, Mg^{2+}, Cl^-, and SO_4^{2-} concentrations were 11.51, 32.95, 326.29, and 377.31 mg/L, respectively.

Author Contributions: S.-Y.L., R.-Z.Z., Q.G. and X.-C.Q. played an important role in this study and upheld a research learning attitude in conducting the experiments, writing, and revising. The experiment was conducted by R.-Z.Z. and supervised by X.-C.Q. All authors have read and agreed to the published version of the manuscript.

Funding: This research was funded by the National Natural Science Foundation of China grant number 31560723 and Ningxia University first-class discipline (water conservancy engineering) construction subsidy project grant number NXYLXK2021A03.

Institutional Review Board Statement: No applicable.

Informed Consent Statement: No applicable.

Data Availability Statement: The data are not publicly available due to privacy.

Acknowledgments: This material is based on work supported by the National Natural Science Foundation of China under award number 31560723 and Ningxia University first-class discipline (water conservancy engineering) construction subsidy project under award number NXYLXK2021A03.

Conflicts of Interest: The authors declare that there was no conflict of interest or any potential financial or other interests that could be perceived to influence the outcomes of this research.

References

1. Lundholm, N.; Moestrup, O. The biogeography of harmful algae. In *Ecology of Harmful Algae*; Graneli, E., Turner, J.T., Eds.; Springer: Berlin, Germany, 2006; Volume 189, pp. 23–35.
2. Southard, G.M.; Fries, L.T.; Barkoh, A. *Prymnesium parvum*: The Texas Experience1. *J. Am. Water Res. Assoc.* **2010**, *46*, 14–23. [CrossRef]
3. Hambright, K.D.; Zamor, R.M.; Easton, J.D.; Glenn, K.L.; Remmel, E.J.; Easton, A.C. Temporal and spatial variability of an invasive toxigenic protist in a North American subtropical reservoir. *Harmful Algae* **2010**, *9*, 568–577. [CrossRef]

4. Bertin, M.J.; Zimba, P.V.; Beauchesne, K.R.; Huncik, K.M.; Moeller, P.D.R. Identification of toxic fatty acid amides isolated from the harmful alga *Prymnesium parvum* carter. *Harmful Algae* **2012**, *20*, 111–116. [CrossRef]
5. Vasas, G.; M-Hamvas, M.; Borics, G.; Gonda, S.; Máthé, C.; Jámbrik, K.; Nagy, Z.L. Occurrence of toxic *Prymnesium parvum* blooms with high protease activity is related to fish mortality in Hungarian ponds. *Harmful Algae* **2012**, *17*, 102–110. [CrossRef]
6. Manning, S.R.; La Claire Ii, J.W. Isolation of polyketides from *Prymnesium parvum* (Haptophyta) and their detection by liquid chromatography/mass spectrometry metabolic fingerprint analysis. *Anal. Biochem.* **2013**, *442*, 189–195. [CrossRef] [PubMed]
7. Zhang, Y.F. The formation, harm and control of 3 common single algae in northern culture ponds. *Jiangxi Aquat. Technol.* **2016**, *4*, 39–40. [CrossRef]
8. He, S. *Effect of Calcium Ion on the Competition among Four Freshwater Algae Species Under Different Nutrient Conditions*; Xi'an University of Technology: Xi'an, China, 2020.
9. Liang, X. *Study on Effects of Several Heavy Metal Ions on Algal Cell Growth*; Shanxi Universiy: Taiyuan, China, 2016.
10. Zhang, Q.; Hu, G. Effect of nitrogen to phosphorus ratios on cell proliferation in marine micro algae. *Chin. J. Oceanol. Limnol.* **2011**, *29*, 739–745. [CrossRef]
11. Chiranjeevi, P.; Mohan, S.V. Critical parametric influence on microalgae cultivation towards maximizing biomass growth with simultaneous lipid productivity. *Renew. Energy* **2016**, *98*, 64–71. [CrossRef]
12. Wu, Z.; Duangmanee, P.; Zhao, P.; Juntawong, N.; Ma, C. The Effects of Light, Temperature, and Nutrition on Growth and Pigment Accumulation of Three *Dunaliella salina* Strains Isolated from Saline Soil. *Jundishapur J. Microbiol.* **2016**, *9*, e26732. [CrossRef]
13. Fournier, E.; Adam-Guillermin, C.; Potin-Gautier, M.; Pannier, F. Selenate bioaccumulation and toxicity in Chlamydomonas reinhardtii: Influence of ambient sulphate ion concentration. *Aquat. Toxicol.* **2010**, *97*, 51–57. [CrossRef]
14. Ma, J.-M.; Cai, L.-L.; Zhang, B.-J.; Hu, L.-W.; Li, X.-Y.; Wang, J.-J. Acute toxicity and effects of 1-alkyl-3-methylimidazolium bromide ionic liquids on green algae. *Ecotoxicol. Environ. Saf.* **2010**, *73*, 1465–1469. [CrossRef] [PubMed]
15. Dao, L.H.T.; Beardall, J. Effects of lead on growth, photosynthetic characteristics and production of reactive oxygen species of two freshwater green algae. *Chemosphere* **2016**, *147*, 420–429. [CrossRef]
16. Cheng, J.; Qiu, H.; Chang, Z.; Jiang, Z.; Yin, W. The effect of cadmium on the growth and antioxidant response for freshwater algae *Chlorella vulgaris*. *SpringerPlus* **2016**, *5*, 1290. [CrossRef] [PubMed]
17. Ren, H.-Y.; Liu, B.-F.; Kong, F.; Zhao, L.; Xie, G.-J.; Ren, N.-Q. Enhanced lipid accumulation of green microalga *Scenedesmus* sp. by metal ions and EDTA addition. *Bioresour. Technol.* **2014**, *169*, 763–767. [CrossRef]
18. Lohman, E.J.; Gardner, R.D.; Pedersen, T.; Peyton, B.M.; Cooksey, K.E.; Gerlach, R. Optimized inorganic carbon regime for enhanced growth and lipid accumulation in *Chlorella vulgaris*. *Biotechnol. Biofuels* **2015**, *8*, 82. [CrossRef]
19. Islami, H.R.; Assareh, R. Enhancement effects of ferric ion concentrations on growth and lipid characteristics of freshwater microalga *Chlorococcum oleofaciens* KF584224.1 for biodiesel production. *Renew. Energy* **2020**, *149*, 264–272. [CrossRef]
20. Roelke, D.L.; Brooks, B.W.; Grover, J.P.; Gable, G.M.; Schwierzke-Wade, L.; Hewitt, N.C. Anticipated human population and climate change effects on algal blooms of a toxic haptophyte in the south-central USA. *Can. J. Fish. Aquat. Sci.* **2012**, *69*, 1389–1404. [CrossRef]
21. Guan, J.; Han, C.; Guan, Y.; Zhang, S.; Yun, J.; Yao, S. Optimizational production of phenyllactic acid by a *Lactobacillus buchneri* strain via uniform design with overlay sampling methodology. *Chin. J. Chem. Eng.* **2019**, *27*, 418–425. [CrossRef]
22. Feng, Z.-K.; Niu, W.-J.; Cheng, C.-T. Optimizing electrical power production of hydropower system by uniform progressive optimality algorithm based on two-stage search mechanism and uniform design. *J. Clean. Prod.* **2018**, *190*, 432–442. [CrossRef]
23. Yang, J.; Li, L.; Yang, L.; Li, J. Uniform design for the parameters optimization of pin-fins channel heat sink. *Appl. Therm. Eng.* **2017**, *120*, 289–297. [CrossRef]
24. Lu, D. Preservation technology of solid medium for algae species such as *Chrysanthemum algae* and *Chaetoceros* spp. *Aquaculture* **2003**, *6*, 5–6.
25. Fang, K.-T.; Lin, D.K.J.; Winker, P.; Zhang, Y. Uniform Design: Theory and Application. *Technometrics* **2000**, *42*, 237–248. [CrossRef]
26. Li, T.Z.; Yang, X.L. An efficient uniform design for Kriging-based response surface method and its application. *Comput. Geotech.* **2019**, *109*, 12–22. [CrossRef]
27. Yan, G.; Zhihong, W.; Keshu, L.; Lifan, L.; Yu, T. Effects of four nutrients on proliferation of *Anabaena aquae* and *Scenedesmus quadricanda*. *Chin. J. Environ. Eng.* **2015**, *9*, 2113–2118. [CrossRef]
28. Zhang, S.; Liu, P.; Wang, Y. Effects of concentrations of iron, calcium and magnesium on the growth and lipid accumulation of microalgal strain *Desmodesmus* sp. WC08. *Guangdong Agric. Sci.* **2014**, *4*, 126–130.
29. Zhang, F.; Liu, T. The Ratio of $Na^+/Mg^{(2+)}$, $Cl^-/SO_4^{(2-)}$ in Brine Effect the Growth of Halotolerant *Dunaliella viridis*. *J. Salt Chem. Ind.* **2010**, *39*, 31–34. [CrossRef]
30. Wang, J.; Liang, S.; Chen, F. Effects of mineral salt on the growth and accumulation in *Crypthecodinium cohnii*. *J. Zhanjiang Ocean Univ.* **2001**, *21*, 18–21.
31. Wang, X.; Huang, X.; Yang, B. Effects of $NaHCO_3$ and Culture Phase on Growth, Protein Content and Fatty Acid Composition of *Isochrysis galbana*. *J. Shandong Agric. Univ. Nat. Sci. Ed.* **2016**, *47*, 345–352.
32. Li, Y.; Zhong, J.; Zheng, M.; Zhuo, P.; Xu, N. Photoperiod mediates the effects of elevated CO_2 on the growth and physiological performance in the green tide alga *Ulva prolifera*. *Mar. Environ. Res.* **2018**, *141*, 24–29. [CrossRef]
33. Baker, J.W.; Grover, J.P.; Brooks, B.W.; Ureña-Boeck, F.; Roelke, D.L.; Errera, R.; Kiesling, R.L. Growth and toxicity of *Prymnesium parvum* (haptophyta) as a function of salinity, light, and temperature 1. *J. Phycol.* **2007**, *43*, 219–227. [CrossRef]

34. Shukla, B.; Rai, L.C. Potassium-induced inhibition of photosynthesis and associated electron transport chain of Microcystis: Implication for controlling cyanobacterial blooms. *Harmful Algae* **2006**, *5*, 184–191. [CrossRef]
35. Pancha, I.C.K.; Ghosh, T.; Paliwal, C.; Maurya, R.; Mishra, S. Bicarbonate supplementation enhanced biofuel production potential as well as nutritional stress mitigation in the microalgae *Scenedesmus* sp. CCNM 1077. *Bioresour. Technol.* **2015**, *193*, 315–323. [CrossRef] [PubMed]
36. White, D.A.; Pagarette, A.; Rooks, P.; Ali, S.T. The effect of sodium bicarbonate supplementation on growth and biochemical composition of marine microalgae cultures. *J. Appl. Phycol.* **2013**, *25*, 153–165. [CrossRef]
37. El-Ansari, O.; Colman, B. Inorganic carbon acquisition in the acid-tolerant alga *Chlorella kessleri*. *Physiol. Plant.* **2015**, *153*, 175–182. [CrossRef] [PubMed]
38. Aomchad, V.; Cristòfol, À.; Della Monica, F.; Limburg, B.; D'Elia, V.; Kleij, A.W. Recent progress in the catalytic transformation of carbon dioxide into biosourced organic carbonates. *Green Chem.* **2021**, *23*, 1077–1113. [CrossRef]
39. Summerfelt, S.T.; Zühlke, A.; Kolarevic, J.; Reiten, B.K.M.; Selset, R.; Gutierrez, X.; Terjesen, B.F. Effects of alkalinity on ammonia removal, carbon dioxide stripping, and system pH in semi-commercial scale water recirculating aquaculture systems operated with moving bed bioreactors. *Aquac. Eng.* **2015**, *65*, 46–54. [CrossRef]
40. Yeh, K.L.; Chang, J.S.; Chen, W.M. Effect of light supply and carbon source on cell growth and cellular composition of a newly isolated microalga *Chlorella vulgaris* ESP-31. *Eng. Life Sci.* **2010**, *10*, 201–208. [CrossRef]
41. Shi, J.Q.; Wu, Z.X.; Song, L.R. Physiological and molecular responses to calcium supplementation in *Microcystis aeruginosa* (Cyanobacteria). *N. Z. J. Mar. Freshw. Res.* **2013**, *47*, 51–61. [CrossRef]
42. Lili, G.; Wei, Z.; Ming, L. Effect of major cations in water on the growth and polysaccharide contents of *Microcystis aeruginosa*. *Ecol. Environ. Sci.* **2013**, *22*, 1358. [CrossRef]
43. Qian, L.I.; Yan-You, W.U.; Liang, Y.J.; Yun-Dong, W.U.; Zhu, H.L. Effects of F^- and Cl^- on Growth of *Chlamydomonas reinhardtii*. *J. Ecol. Rural Environ.* **2015**, *31*, 238–243. [CrossRef]
44. Wang, Q.; Zhang, Y.; Li, A.; Zhang, C. Effects of Sulfur Concentration on the Photosynthetic Physiology and Biocheical Compostion of Scenedesmus Acuminatus. *Acta Hydrobiol. Sin.* **2017**, *41*, 904–913. [CrossRef]
45. Khotimchenko, S.V.; Yakovleva, I.M. Lipid composition of the red alga *Tichocarpus crinitus* exposed to different levels of photon irradiance. *Phytochemistry* **2005**, *66*, 73–79. [CrossRef] [PubMed]